HHS Public Access

Author manuscript

Cell Rep. Author manuscript; available in PMC 2017 December 13.

Published in final edited form as:

Cell Rep. 2017 November 28; 21(9): 2419–2432. doi:10.1016/j.celrep.2017.10.123.

Gamma oscillations in rat hippocampal subregions dentate gyrus, CA3, CA1, and subiculum underlie associative memory encoding

John B. Trimper[1], **Claire R. Galloway**[1], **Andrew C. Jones**[2], **Kaavya Mandi**[2], and **Joseph R. Manns**[1,*]

[1]Department of Psychology, Emory University, Atlanta, GA 30322, USA

[2]Neuroscience and Behavioral Biology Program, Emory University, Atlanta, GA 30322, USA

SUMMARY

Neuronal oscillations in the rat hippocampus relate to both memory and locomotion, raising the question of how these cognitive and behavioral correlates interact to determine the oscillatory network state of this region. Here, rats freely locomoted while performing an object-location task designed to test hippocampus-dependent spatial associative memory. Rhythmic activity in theta, beta, slow gamma, and fast gamma frequency ranges were observed in both action potentials and local field potentials (LFPs) across four main hippocampal subregions. Several patterns of LFP oscillations corresponded to overt behavior (e.g., increased dentate gyrus-CA3 beta coherence during stationary moments and CA1-subiculum theta coherence during locomotion). In comparison, slow gamma (~40 Hz) oscillations throughout the hippocampus related most specifically to object-location associative memory encoding rather than overt behavior. The results help to untangle how hippocampal oscillations relate to both memory and motion, and single out slow gamma oscillations as a distinguishing correlate of spatial associative memory.

Graphical Abstract

*Lead Contact: Joseph R. Manns, Ph.D., Department of Psychology, Emory University, 36 Eagle Row, Atlanta, GA 30322, 404-727-7459, jmanns@emory.edu.

AUTHOR CONTRIBUTIONS: J.B.T. and J.R.M. designed experiments and analyses; J.B.T. conducted experiments and analyses; C.R.G. and K.M. assisted with data collection. A.C.J. and K.M. assisted with data processing. J.B.T. and J.R.M. wrote the manuscript.

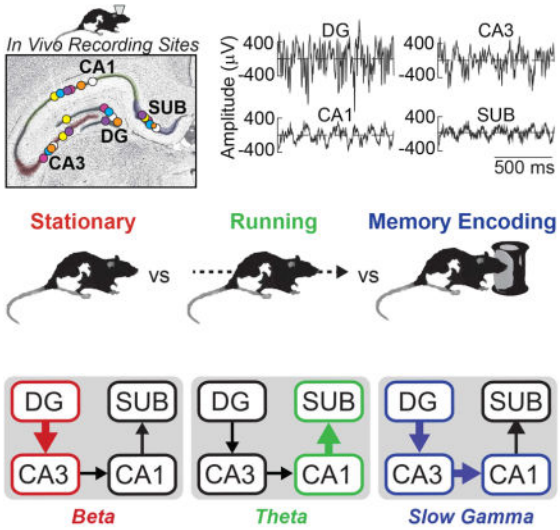

Keywords

Memory; Hippocampus; Object; Synchrony; Electrophysiology

Introduction

Neuronal oscillations reflect rhythmic fluctuations of transmembrane ion currents summed across neurons (Buzsaki et al., 2012). This rhythmicity modulates the timing—and thus efficacy—of synaptic transmission and synaptic plasticity (Huerta & Lisman, 1993; Hyman et al., 2003; Orr et al., 2001; Zarnadze et al., 2016), shaping interactions between populations of neurons within and across brain regions (Engel et al., 2001; Fries, 2015; Singer, 1999; Varela et al., 2001). Depending on the brain region, oscillatory activity often correlates with overt behaviors, such as reaching or locomotion (Ahmed & Mehta, 2012; MacKay & Mendonca, 1995), or with covert cognition, such as attention (Tiitinen et al., 1993; Tallon-Baudry et al., 1997; Fries et al., 2001; Jensen et al., 2007) or memory (Igarashi et al., 2014; Montgomery & Buzsaki, 2012; Jutras et al., 2009, 2013; Shirvalkar et al., 2010; Trimper et al., 2014). Much progress has been made in understanding how neuronal oscillations in sensory (Brovelli et al., 2004; Nicolelis et al., 1995), motor (Engel & Fries, 2010; MacKay & Mendonca, 1995), and cognitive (Herrmann et al., 2004; Colgin, 2016) systems relate to the respective functions of these systems by mediating well-timed interactions within and across neuronal networks. A major remaining challenge is to understand how multiple neuronal oscillations with differing cognitive and behavioral correlates can interact to determine the oscillatory network state of a brain region.

One brain region exhibiting oscillatory activity correlated with both cognition and overt behavior is the hippocampus. In particular, neuronal oscillations in the hippocampus relate closely to both memory and movement (Colgin, 2016, for review). For example, in the rodent hippocampus, local field potential (LFP) oscillations in the theta (6–10 Hz), slow gamma (30–55 Hz), and fast gamma (65–90 Hz) frequency ranges relate not only to memory

performance but also to running speed outside of explicit memory tasks (Kemere et al., 2013; Slawinska & Kasicki, 1998; Trimper et al., 2014; Winson, 1978; Zheng et al., 2016). Despite our good understanding of the relationship between hippocampal oscillations and locomotion, other important behaviors are underexplored. In semi-naturalistic settings, rats explore their environment in sporadic bursts of running, punctuated by frequent stops during which they often explore their surroundings, including the objects they would ordinarily encounter in real-world settings (Golani et al., 1993; Renner and Seltzer, 1991; Whishaw et al., 2006). However, very little is known about the patterns of hippocampal oscillations during these moments of spontaneous exploration. This gap in knowledge about hippocampal oscillations during object exploration contrasts with the increasing use of spontaneous object recognition memory tasks in rodent studies (Clark and Squire, 2010) and with the widely-held view of the mammalian hippocampus as being central to associating nonspatial items, such as objects, with spatial information, such as locations (e.g., Davachi, 2006; Knierim et al., 2006; Manns & Eichenbaum, 2006; Witter et al., 2000). Thus, an important question is how the patterns of oscillations in the hippocampus distinguish object exploration from other behaviors during spatial navigation and whether these oscillatory patterns relate to encoding object-location associative memories or more narrowly reflect the act of exploration.

To address this broad question, we recorded neuronal activity from the hippocampus as rats were tested for object-location associative memory while freely locomoting on a circular track. The specific questions were: 1) whether patterns of hippocampal oscillations during exploration of objects would reflect more than the cessation of locomotion, and if so, 2) the extent to which these oscillations would correspond to memory for the object encounters rather than simply reflecting the act of exploration. We recorded spiking and LFPs from the principal cell layers of four major subregions of the hippocampus: dentate gyrus (DG), CA3, CA1, and subiculum. The goal in recording from all four regions simultaneously was to measure the functional dynamics of the local circuitry and assess potential heterogeneity across regions in terms of correlates with cognition and behavior. For example, by one view, dentate gyrus and CA3 are hypothesized to be particularly important for associative memory encoding, whereas CA1 and subiculum may be of greater importance for resolving discrepancies between internal and external representations in service of environmental navigation (Kesner & Rolls, 2015).

The results showed that the pattern of oscillatory activity across these four subregions clearly distinguished overt behaviors, differing prominently between moments of object exploration, stationary moments, and periods of locomotion. Moreover, when the pattern of oscillatory activity was contrasted across memory conditions during the single behavioral state of object exploration, slow gamma power and region-region coherence distinguished between exploring novel, repeated, and repositioned objects and, during exploration of novel objects, related to whether the rat would subsequently show good object-location associative memory. The results highlight the intersection of memory and locomotion in determining the oscillatory network state of the hippocampus and offer insights as to how oscillatory signatures of both behavior and cognition interact within a single brain region. The results also reveal that slow gamma oscillations across the major hippocampal subregions mark an oscillatory network state of effective associative memory encoding.

Results and Discussion

To ask how hippocampal network activity related to both memory and overt behavior, action potentials and LFPs were recorded simultaneously from DG, CA3, CA1, and subiculum in six rats as the animals performed a novel object recognition memory task that probed rats' memory for objects and objects' locations. Figure 1 shows LFP recording sites in each of the four subregions in six rats, as well as example LFPs recorded from each of these four subregions during the approach and exploration of novel objects. The intra-hippocampal connectivity between DG, CA3, CA1, and subiculum is serial (Amaral & Witter, 1989), and thus a key initial question was how the oscillatory amplitude and synchrony between LFPs of connected subregions changed as rats engaged in object exploration behavior. Accordingly, Figure 1 also shows power and coherence during object approach and exploration (mean number of object encounters ± SEM across rats = 50.8 ± 8.6 events) across a broad range of frequencies between LFPs from connected regions (DG-CA3, CA3-CA1, and CA1-subiculum). Large increases in slow gamma coherence between DG and CA3 and between CA3 and CA1 are apparent during novel object exploration. Increases in slow gamma power during object exploration relative to the pre-exploration approach period are also visible in these regions. A main question of the present study is the extent to which this pattern of intra-hippocampal oscillatory synchrony reflected memory for the object encounters or simply the act of object exploration. However, as hippocampal activity is well known to be modulated by voluntary locomotion (Whishaw and Vanderwolf, 1973), a preliminary question was whether the pattern of oscillatory interactions observed actually reflected object exploration or just the cessation of locomotion.

Novel Object Exploration Elicited a Distinct Hippocampal Oscillatory State

As shown in Supplemental Figure S1 for DG, CA3, CA1, and subiculum (and in previous reports for subsets of these subregions, e.g., Ahmed & Mehta, 2012; Kemere et al., 2013; Zheng et al., 2015), the frequency and amplitude of hippocampal LFPs—in theta, slow gamma, and fast gamma ranges—are strongly influenced by the rat's speed of locomotion. Notably, slow gamma power was at its relative highest across movement speeds in DG, CA3, and CA1 when a rat was stationary. Thus, a possible explanation for the slow gamma coherence increase observed between DG and CA3 and between CA3 and CA1 (as well as power increases within those regions) during object exploration is that the rats stopped locomoting.

To assess this possibility, power and coherence were calculated for hippocampal LFPs during novel object exploration events (mean number of events ± SEM across rats = 50.8 ± 8.6), stationary moments when the rat was not exploring objects (78.7 ± 26.5), locomotion as a rat approached novel objects (50.8 ± 8.6), and locomotion not close in time to object exploration (168.2 ± 18.9; see Experimental Procedures for details on how these epochs were defined and see Supplemental Figure S1 for confirmation that average speed of movement differed across these four behavioral states). Figure 2 shows subregional power and coherence across the four behavioral conditions (approach, exploration, stationary, and running). The results are also shown after subtracting the grand mean across behavioral conditions to highlight better the similarities and dissimilarities between conditions in a

manner that paralleled the statistical testing (and removed the 1/f trend from the spectral measures). Specifically, differences in spectral measures between conditions were evaluated by an ANOVA-based statistical approach that tested if data from at least one condition differed from the grand mean. Table S1 provides the accompanying statistics for each significant frequency range (frequency cluster) derived from a cluster-based random permutation approach (see Materials and Methods for details of analyses). Figure S2 reproduces the data displayed in Figure 2 but includes only frequencies below 20 Hz to enhance visualization of differences in this lower frequency range. The results show that hippocampal oscillatory activity during object exploration differed markedly from hippocampal activity during locomotion and, importantly, also from hippocampal activity during stationary moments. This latter finding indicates that the hippocampal oscillatory network state during object exploration could not be accounted for merely as a reduction in locomotive speed, instead supporting the idea that hippocampal subregions were engaged in a unique pattern of oscillatory activity that was specific to object exploration.

In particular, object exploration was distinguished from the other behavioral conditions by especially prominent slow gamma (30–55 Hz) and fast gamma (65–90 Hz) power in DG, CA3, and CA1, consistent with a previous report (Trimper et al., 2014). Stationary moments were distinguished by relatively high beta (13–25 Hz) power in DG and CA3, as well as relative decreases in fast gamma power in CA1 and subiculum and in theta power in all four subregions. The oscillatory patterns associated with stationary moments are consistent with previous studies that reported changes associated with cessation of locomotion (Ahmed & Mehta, 2012; Kemere et al., 2013; Zheng et al., 2015; though Rangel et al., 2015 observed increases in DG beta only when cessation of locomotion occurred at behaviorally relevant locations). The two conditions involving locomotion (i.e., approaching an object or running on a track with no object present) were similar to one another and were distinguished from the other conditions by lower levels of (and perhaps somewhat lower frequency) slow gamma power (relative to object exploration), particularly in DG and CA3, and by high levels of theta power, particularly in CA1 and subiculum. In addition to power, LFP synchrony between connected hippocampal regions, as measured with coherence, also distinguished object exploration from the other behavioral conditions. Object exploration was associated primarily with large relative increases in slow gamma coherence between DG and CA3, and between CA3 and CA1. Stationary moments were associated with relatively high beta coherence between DG and CA3. Theta coherence between CA1 and subiculum was similarly high for both locomotive states relative to the other two behavioral conditions. Thus, distinct overt behaviors were associated with markedly different patterns of oscillatory activity throughout the hippocampal subregions and the pattern of activity observed during object exploration—namely, prominent slow gamma in DG, CA3, and CA1—could not be accounted for merely as the product of locomotive speed.

Theta, slow gamma, and fast gamma oscillations were prominent in the hippocampal LFPs recorded in the present study, and prior studies of hippocampal oscillations have observed that the amplitude of gamma oscillations can be modulated by the phase of theta oscillations (e.g., Tort et al., 2009; Trimper et al., 2014). We therefore next asked if the magnitude of the theta-phase modulation of slow gamma or fast gamma amplitude differed between behavioral conditions in DG, CA3, CA1, or subiculum. The magnitude theta-phase

modulation was calculated separately for slow gamma and fast gamma as a modulation index based on the LFP in each region as described previously (e.g., Tort et al., 2009). Figure S3 shows the results as mean modulation indices across rats for each region and for each behavioral condition. The amplitudes of both slow gamma and fast gamma were modulated by the phase of theta oscillations in DG, CA3, CA1, and subiculum, but the modulation indices in each region were similar across behavioral conditions (exploration, stationary, run, and approach). Specifically, one-way ANOVAs for slow gamma and for fast gamma within each region observed no main effects of behavioral condition (all ps > 0.10). Thus, although the patterns of theta and gamma oscillations as measured by power and coherence differed across behavioral states, the extent to which slow gamma and fast gamma oscillations were modulated by the phase of theta did not.

As an additional control analysis to rule out cessation of locomotion as the primary driver of the prominent gamma increases during object exploration, slow gamma and fast gamma power and coherence were calculated across time relative to onset of object exploration (mean number of events ± SEM across rats = 50.8 ± 8.6) and to offset of locomotion when no objects were present (i.e., 2 s of locomotion followed by 2 s of remaining stationary; 17.0 ± 4.6 events). Figure 3 shows these data in addition to differences in average locomotion speed. When rats stopped to explore objects as compared to when rats simply stopped, gamma power and coherence, particularly slow gamma in DG and CA3, was markedly and significantly higher (see Table S2 for detailed statistics). The amount of head movement during object exploration was somewhat greater than during stationary moments (Figure 3A), further indicating that the increased slow gamma power and coherence during exploration was not simply related to the negative correlation between movement speed and slow gamma power (e.g., Supplemental Figure 1). Fast gamma power in all subregions and fast gamma coherence between CA3 and CA1 were also revealed to increase significantly during object exploration. However, these fast gamma differences could potentially be accounted for by locomotive speed differences. Taken together, these results indicate that the pattern of hippocampal LFP activity during object exploration represents a distinct network state and demonstrate that the high levels of slow gamma oscillations reflect more than the cessation of locomotion.

Hippocampal Spike Timing Was Modulated by Oscillations

An important component of oscillatory analyses is the demonstration of spiking modulation by rhythmic LFP activity, which would indicate that oscillations in LFPs were attributable to local circuits and could not instead be attributed to volume conduction from distal sources (Buzsaki et al., 2012). Therefore, to assess the extent to which oscillations in hippocampal LFPs modulated spike timing within and between subregions, action potentials from principal neurons in each subregion were compared to simultaneously recorded LFPs in each region (e.g., DG spikes and DG LFPs) as well as to simultaneously recorded LFPs in downstream connected regions (e.g., DG spikes and CA3 LFPs). Across the entire recording session, regardless of behavioral state, the overall trend was that spike timing for a substantial portion of neurons in all four subregions (see Table S3) was significantly phase-aligned to multiple oscillatory ranges (theta, beta, slow gamma, and/or fast gamma), both in the same subregion (Figure 4) and in the immediate downstream region (Figure S4). Only

neurons firing at least 50 action potentials when oscillatory power was strong were considered to address the possibility that spike-phase relationships could be obscured by including spikes in the analyses when oscillations were not prominent. The analysis was conducted separately for each frequency range (theta, beta, slow gamma, and fast gamma). The results indicated that the timing of action potentials of principal neurons of the hippocampus were modulated by oscillations in each frequency range but that the extent of modulation depended on the specific range and hippocampal subregion. In addition, the phase at which spiking tended to occur relative to oscillations the LFP also depended on the specific frequency range and hippocampal subregion (see Figure 4 and Figure S4). In particular, action potentials of significantly phase-modulated principal cells in DG and CA3 were both more likely to be aligned to the peak of local slow gamma oscillations yet both more likely to be aligned to the trough of local fast gamma oscillations (Watson-Williams F Test of phases for slow gamma vs. fast gamma; DG: $F(1,47) = 76.35$, $p < .0001$; CA3: $F(1,137) = 318.5$, $p < .0001$). More broadly, the findings suggest that the LFP oscillations reflect physiologically-relevant signals in the hippocampus.

In comparison to LFP oscillations, hippocampal spiking activity as measured by either firing rates (Figure S5) or spike-phase timing (Figures 4 and S4) only modestly distinguished behavioral states, perhaps reflecting an advantage for LFPs in summing activity across many neurons to assess network states (Buzsaki et al., 2012). In particular, a significant difference in firing rate across behaviors, after Bonferroni alpha correction for four subregions, was revealed in CA1 [$n = 266$, $F(3,795) = 18.65$, $p = <0.0001$, partial $eta^2 = .066$] and DG [$n = 40$; $F(3,117) = 4.356$, $p = 0.006$, partial $eta^2 = 0.006$), but not in CA3 [$n = 124$, $F(3,369) = 2.263$, $p = 0.081$, partial $eta^2 = 0.0181$], or subiculum [$n = 39$; $F(3,114) = 0.721$, $p = 0.542$, partial $eta^2=0.019$]. Modestly higher CA1 pyramidal neuron firing rates were associated with locomotion, consistent with previous reports (e.g., Ahmed & Mehta, 2012; Zheng et al., 2015), whereas putative DG granule cells preferably fired during Exploration relative to other behavioral states.

In terms of spike-phase timing, low hippocampal firing rates overall (mean Hz ± SEM: DG = 0.79 ± 0.12; CA3 = 0.63 ± 0.07; CA1 = 0.87 ± 0.45; SUB = 1.09 ± 0.12) prevented analyses regarding differences in spike timing across behavioral conditions for ranges other than the theta range, as spike-phase modulation by transient or nonstationary rhythms can be assessed only when spikes are present and oscillatory bouts are pre-selected to be strong to avoid spurious results (Colgin et al., 2009). These analyses of spike to theta phase modulation by behavioral state (Figure S5) revealed no significant differences in terms of the number of significantly phase modulated neurons across states, at least not after Bonferroni correction for four subregions [DG: χ^2 (3) = 5.946; CA3: $\chi^2(3) = 8.682$, $p = 0.035$; CA1(3): $\chi^2(3) = 03.316$, $p = 0.345$; SUB: $\chi^2(3) = 4.110$, $p = 0.250$], but did show a significant increase in the strength of theta phase alignment (i.e., pairwise phase consistency; Vinck et al., 2010) for locomotive relative to non-locomotive states for DG [$F(3,53) = 7.02$, $p < 0.001$, partial $eta^2 = 0.397$]. Thus, spiking in all hippocampal regions was modulated by oscillations in all four oscillatory ranges (Figure 4), but analytical constraints permitted assessment of spike-phase differences between behavioral conditions for only the theta range. As a result, subsequent analyses focused on whether oscillations in LFPs across subregions of the hippocampus during object exploration reflected memory for the

encounters or just the behavioral state of exploration, an approach that revealed marked oscillatory differences during object exploration (Figures 1–3) and that was not limited by the analytical constraints that pertained to spiking.

Hippocampal Slow Gamma Oscillations during Object Exploration Distinguished Memory Conditions in an Object-Location Associative Memory Task

A main question of the present study was whether patterns of hippocampal oscillations would correspond to associative memory for the object encounters. Figure 5 shows a schematic of and behavioral results from the object-location recognition memory task, which involved up to 24 trials per session of rats completing triplets of clockwise laps on a circle track and spontaneously exploring novel objects, objects repeated in the same location, and objects repeated in swapped locations. Rats exhibit a well-known preference for novelty (Ennaceur and Delacour, 1988), and thus a reduction in exploration time across successive encounters with a stimulus can be interpreted as rats remembering the stimulus. Indeed, rats showed a large and significant reduction in exploration duration [$t(5) = 4.50$, $p = 0.006$, Cohen's $d = 1.836$] when novel objects from lap 1 were encountered again in the same locations on lap 2 (mean number of events ± SEM across rats = 87.0 ± 10.1), which indicated memory for at least the object identities. To ask if the rats also remembered the specific locations of the objects, on some trials the objects were repeated again in swapped locations on lap 3. Rats explored these swapped objects (mean number of events ± SEM across rats = 80.7 ± 5.6) for a different amount of time than repeated (20.3 ± 1.4 events) or novel objects (n = 20.3 ± 1.4 events) in control conditions [$F(2,10) = 10.93$, $p = 0.003$, partial $eta^2 = 0.686$]. Specifically, rats explored swapped objects for a longer duration than objects repeated in the same location [$t(5) = 3.45$, $p = 0.018$, $d = 1.41$] but less than novel objects on lap 3 [$t(5) = 3.20$, $p = 0.024$, $d = 1.30$], indicating that rats had memory for the prior locations of objects, similar to previous reports (e.g., Save et al., 1992).

To ask if hippocampal oscillations might differ by memory condition, power and coherence across subregions were calculated during the first second of lap 3 object exploration of repeated, novel, and swapped objects lasting at least 1 second, when overt movement was similar (see Figure S1). A window of 1 second rather than a longer duration (e.g., 2 seconds) was selected to permit inclusion of a number of events from each condition in the analyses (mean number of events ± SEM across rats = 10.0 ± 1.1, 4.2 ± 0.9, and 27.8 ± 4.9 for novel objects, repeated objects, and swapped objects on lap 3, respectively). Figure 6 shows the results across frequency ranges as differences from the grand mean across conditions to highlight the comparisons of interest (see Table S4 for detailed statistics; see Figure S6 for figures that include individual data points for each rat). Slow gamma power in DG and CA3 differed markedly across the three memory conditions, in both cases being at its relative highest during exploration of novel objects, its relative lowest during exploration of repeated objects, and at an intermediate level during exploration of swapped objects. Based on the overall prominence of hippocampal gamma oscillations during object exploration (e.g., Figure 2), power in each subregion was also averaged and plotted separately in the slow gamma range and fast gamma range as normalized differences across the three memory conditions. Statistically significant linear trends (novel>swap>repeat) were observed for overall average hippocampal slow gamma power [$F(1,5) = 15.60$, $p = 0.011$, partial eta^2 =

0.757] and for DG [F(1,5) = 28.46, p = 0.003, partial eta^2 = 0.851] and CA3 slow gamma power specifically [F(1,5) = 16.80, p = 0.009, partial eta^2 = 0.771], whereas no significant differences were observed for any contrast in the fast gamma range (see Figure 6 and Table S5 for statistical details).

As compared to the results for power, coherence between connected hippocampal subregions showed relatively small differences across memory conditions, at least when plotted across a broad range of frequencies (Figure 6). However, when coherence between subregions was averaged across the slow gamma range, statistically significant linear trends (novel>swap>repeat) were observed for overall hippocampal slow gamma coherence [F(1,5) = 11.85, p = 0.018, partial eta^2 = 0.703] as well as for the slow gamma coherence between CA1 and subiculum specifically [F(1,5) = 6.70, p = 0.046, partial eta^2 =0.583]. To ask if these results for coherence could be explained by simultaneous but undirected increases in slow gamma power (e.g., due to volume conduction) the non-normalized directed transfer function (DTF) was calculated and plotted for oscillatory interactions between hippocampal subregions for the three memory conditions. DTF is a directional autoregressive metric (similar to Granger causality in the frequency domain) that discounts zero-lag phase relationships and instead reflects the predictiveness of oscillations in one region for oscillations of the same frequency in another region (Kaminski & Blinowska, 1991). Statistically significant linear trends (novel>swap>repeat) were observed for overall hippocampal slow gamma DTF [F(1,5) = 19.01, p = 0.007, partial eta^2 = 0.795] as well as for the DTF between DG and CA3 specifically [F(1,5) = 8.01, p = 0.037, partial eta^2 = 0.616]. No significant differences between memory conditions were observed in the fast gamma range for power, coherence, or DTF (zero of thirteen linear contrasts in panels C–E of Figure 6; see Table S5 for detailed statistics). In contrast, seven of the thirteen linear contrasts for slow gamma power, coherence, and DTF (Figure 6, panels C–E) were statistically significant, a proportion higher than one would expect by chance with an alpha level of 0.05 (see Figure 6 for clarification of alpha corrections for multiple comparisons).

Thus, the results demonstrated increased slow gamma activity in a subset of hippocampal subregions correlated with the degree of novelty associated with the lap 3 object presentations. In particular, novel objects were associated with the largest slow gamma amplitude, synchrony, and predictiveness. In comparison, repeated objects in novel locations were associated with the second highest levels, and repeated objects in repeated locations were associated with the lowest levels. These results support a role for hippocampal slow gamma oscillations in the encoding of novel associative recognition memories for objects and their locations.

Hippocampal Slow Gamma Oscillations during Exploration of Novel Objects Related to Subsequent Memory for Objects and Locations

The pattern of slow gamma differences observed during the lap 3 test of object-location associative memory (novel>swap>repeat) suggested that the degree of slow gamma might have been inversely related to the amount of information repeated from the initial object presentation, and thus, perhaps positively related to the amount of new encoding at the time of test. To ask more directly if hippocampal oscillations would reflect memory encoding,

LFPs recorded during lap 1 novel object exploration were split into three subsequent memory conditions based on whether, on laps 2 and 3, the rats showed good memory for both the object and its location ("object+location"), good memory for the object but not its location ("object"), or poor memory for both aspects of the initial encounter ("poor"). Figure 5 illustrates how the memory conditions were defined and shows performance split by the three subsequent memory conditions. Rats did not decrease their exploration times from lap 1 to lap 2 for the poor memory condition [$t(5) = 0.296$; $p = 0.779$, $d = 0.121$], but decreased their exploration times from lap 1 to lap 2 similarly for object+location [83% reduction; $t(5) = 21.857$; $p < 0.0001$, $d = 8.923$] and object [85% reduction; $t(5) = 51.627$, $p < 0.0001$, $d = 21.08$] memory conditions. On lap 3, rats significantly increased their exploration times for the object+location condition [lap 2 to 3 percent increase = 341%; $t(5) = -3.425$, $p = 0.019$, $d = 1.398$] but did not do so for the object memory condition [lap 2 to 3 percent decrease = 5%; $t(5) = 0.304$; $p = 0.773$, $d = 0.124$]. Thus, the behavioral results validated the partitioning of the events into poor, object, and object+location conditions.

Figure 7 shows differences during the initial 1.5 s of novel object exploration between subsequent memory conditions for power, coherence, and DTF across hippocampal subregions (see Tables S6 and S7 for detailed statistics; see Figure S7 for figures that include individual data points for each rat). A 1.5-s window was used rather than a 2-s window to permit inclusion of enough events in each memory condition (mean number of events ± SEM across rats = 8.5 ± 1.6, 21.5 ± 3.7, and 8.8 ± 2.1 for object+location, object, and poor memory conditions, respectively). Similar to the results for the lap 3 memory test, the subsequent memory contrasts highlighted the slow gamma range. More specifically, average power in the slow gamma range in DG and CA3 differed markedly and statistically significantly across the three memory conditions. For both subregions, slow gamma power was at its relative highest during exploration of novel objects for which both the object and the location were subsequently remembered, its relative lowest during exploration of novel object encounters that were poorly remembered, and at an intermediate level during exploration of novel objects for which the object identity but not the location were remembered [linear trend; DG: $F(1,5)=11.64$, $p=0.019$, partial $eta^2 = 0.699$; CA3: $F(1,5) = 6.835$, $p = 0.047$, partial $eta^2 = 0.578$; overall hippocampus mean: $F(1,5) = 6.835$, $p = 0.047$]. This same pattern (object+location>object>poor) was also present in DG-CA3 coherence [$F(1,5) = 40.294$, $p = 0.001$, partial $eta^2 = 0.890$] and overall hippocampal coherence [$F(1,5) = 14.410$, $p = 0.013$, partial $eta^2 = 0.742$]. The pattern was similar for DTF, although in this case the differences did not reach statistical significance (all ps > 0.142). In comparison, for the fast gamma range, the trends for power, coherence, and DTF were less consistent and were statistically significant for only CA3-CA1 coherence [$F(1,5) = 15.981$, $p = 0.010$, partial $eta^2 = 0.762$]. In sum, five of the thirteen linear contrasts for slow gamma power, coherence, and DTF were statistically significant, a proportion higher than one would expect by chance with an alpha level of 0.05 (see Figure 7 panels C–E).

Thus, combined with the previous results from the lap 3 memory test, the results from lap 1 novel object exploration indicated that the patterns of oscillations in the hippocampus, particularly in the slow gamma range, clearly distinguished moments when the rats were similarly engaged in the behavior of object exploration based on inferred differences in subsequent memory content and quality. In particular, the amount or success of memory

encoding during an object-location associative memory task appeared to be reflected in the general prominence of intra-hippocampal slow gamma oscillatory interactions.

General Discussion

In the present work, we asked whether the patterns of hippocampal oscillations during object exploration in an object-location associative memory task corresponded best to 1) cessation of locomotion, 2) the act of object exploration, or 3) memory for the object encounters. Results indicated that the overall pattern of hippocampal theta, beta, slow gamma, and fast gamma oscillations across DG, CA3, CA1, and subiculum were influenced by all three variables. However, during object exploration, slow gamma oscillations in particular related most specifically to associative memory for the object encounters. Hippocampal LFPs during object exploration were marked by prominent slow gamma oscillations, for which the strength and degree of intra-hippocampal synchrony related to subsequent spatial associative memory for the objects and, likewise, differentiated between bouts of exploring novel, repeated, and relocated objects. These patterns of slow gamma oscillations differed starkly from those observed during both locomotion and during stationary moments. The memory effects on slow gamma oscillations were not limited to oscillatory power in a single hippocampal subregion or to coherence in any one region-region interaction but instead appeared to reflect an increased prevalence of slow gamma oscillations throughout the hippocampus (although not uniformly) during associative memory encoding. Thus, the overall pattern of oscillatory activity in the hippocampus distinguished object exploration as a unique network state, and the specific pattern of hippocampal slow gamma oscillations reflected associative memory for the encounters rather than solely the act of exploration.

One interpretation of the current results is that slow gamma oscillations related specifically to associative encoding of object-location memory in the hippocampus, whereas the other patterns of oscillations, particularly theta, reflected more global interactions between the hippocampus and other brain regions in support of integrating non-memory processes. Previous studies have highlighted slow gamma oscillations in the hippocampus as an indicator of intra-hippocampal synchrony (Colgin et al., 2009; Colgin & Moser, 2010), and a number of studies have highlighted the importance of the hippocampus for spatial associative memory (e.g., Eichenbaum et al., 1999; Komorowski et al., 2009; Tort et al., 2009). In line with these results, prominent intra-hippocampal slow gamma oscillations during exploration of novel objects related to good subsequent memory for both the object and its location and, at test, correlated with the degree of object/location novelty. Oscillations in other frequency ranges were better explained by differences in overt behavior. Theta oscillations are believed to emerge from, and in turn support, interactions between the hippocampus and many other brain regions (Buzsaki, 2002; Colgin, 2016), and theta rhythms within the hippocampal formation are well known to be strongly modulated by locomotive speed (Bender et al., 2015; King et al., 1998; Slawinska & Kasicki, 1998; Whishaw & Vanderwolf, 1973).

The idea offered here is not that theta and slow gamma oscillations in the hippocampus relate narrowly or universally, for example, to locomotion and associative memory encoding, respectively. Indeed, numerous past studies have linked hippocampal theta oscillations and

memory performance, for example, during spatial navigation (Belchior et al., 2014; McNaughton et al., 2006; Siegle & Wilson, 2014; Wang et al., 2015; Winson, 1978), and in the current report, we replicate a clear (inverse) relationship between locomotion and slow gamma oscillations in the rat hippocampus. Further, others have previously made the case that slow gamma oscillations in the hippocampus correspond to memory retrieval processes rather than encoding processes (Colgin et al., 2009; Colgin & Moser, 2010). Instead, the view advanced here is that memory states intersect with behavioral states to shape the oscillatory dynamics of the hippocampus. By this view, during encounters with novel objects —and against the backdrop of oscillations corresponding to that behavioral state—slow gamma oscillations could coordinate spike timing and synaptic plasticity between subregions of the hippocampus in support of associating those objects in memory with the location in which it was encountered as the rats navigated and explored the entire testing apparatus.

More broadly, the current findings highlight the importance of considering object exploration as something more than the cessation of locomotion and how memory for this behavior would be supported by the hippocampus. Many have emphasized the confluence of spatial and nonspatial inputs in the mammalian hippocampus (Knierim et al., 2006; Manns & Eichenbaum, 2006; Witter et al., 2000) and have suggested that it may be particularly important for remembering nonspatial items in a spatial context, such as remembering an object encountered in a particular location (Burgess et al., 2002; Kesner et al., 2004; Jarrard, 1993; Malkova & Mishkin, 2003). Moving forward, additional work will be needed to understand how oscillatory interactions between the hippocampus and other brain regions mediate local and global neural processes needed to negotiate bilaterally between making memories during action and acting on retrieved memories. In this avenue, study of oscillations in the hippocampus can reveal more broadly how action and cognition can combine to shape network dynamics in the brain.

Experimental Procedures

Subjects

Subjects were six male Long-Evans rats aged 6 to 12 months, individually housed (12h light/dark cycle; testing during light phase) with free access to water. Rats were placed on a restricted diet such that the animals maintained at least 90% of their free-feeding weight (~400g). All procedures involving rats were approved by the Institutional Animal Care and Use Committee at Emory University. The Supplemental Experimental Procedures contain additional details for procedures described below.

Behavioral Task and Analyses

Figure 5 shows a schematic of the behavioral task. Each trial consisted of a single lap around the track with no objects present followed by three laps with objects present in the 10 and 2 o'clock positions, relative to the inner stem of the track at 6 o'clock. On the first object lap (lap 1), rats encountered two novel objects. On lap 2, rats encountered duplicates of the same objects from lap 1 in the same positions. On lap 3, rats encountered one of two new object configurations. Either one object was replaced with a duplicate in the same location (Repeat)

while the other was replaced with a novel object (Novel), or the two objects were repeated again, but in swapped locations (Swap). Rats performed up to 72 trials across up to 5 days of testing, with up to 24 trials on a single day. Sessions were recorded using a digital video camera (30 frames/sec), and the rat's head location was recorded for each frame. This frame-by-frame location information was combined with manual coding of object exploration events to define epochs of exploration, stationary moments, and periods of locomotion across a range of movement speeds.

The behavioral data was also used to partition lap 1 exploration events by subsequent memory (see Figure 5). Specifically, lap 1 object encounters lasting at least 1.5-seconds were sorted into memory conditions by subsequent exploration times on laps 2 and 3. Objects for which rats reduced their exploration duration from lap 1 to lap 2 by less than 50% were assigned to the "poor" memory condition. Objects for which rats reduced their exploration from lap 1 to lap 2 by at least 50% and then explored that object more than repeated objects on lap 3 when it swapped locations were assigned to the "object+location" memory condition. If rats reduced their exploration of an object from lap 1 to lap 2 by at least 50%, but then explored the object on lap 3 less than their average exploration time for repeat objects, the object was assigned to the "object" memory condition. Lap 3 exploration was compared to the average exploration duration for repeat objects based on the idea that the lap 3 repeat exploration duration would, on average, represent a combination of object +location memories and object memories.

Surgical Implantation of Tetrodes and Data Acquisition

Sterile-tip surgery was conducted under isoflurane anesthesia to implant chronic recording tetrodes, which were subsequently positioned in the principal cell layers of DG, CA3, CA1, and subiculum subregions of the dorsal hippocampus in one hemisphere. LFPs were recorded continuously (sampling rate = 1,500 Hz; bandpass filter = 1–400 Hz). Spiking data were recorded (sampling rate = 30,000 Hz; bandpass = 600–6000 Hz) for putative action potentials that surpassed a user-defined amplitude threshold. Action potentials recorded on the same tetrode were later manually separated into distinct units by plotting several waveform characteristics across the four wires (e.g., peak spike amplitude, waveform shape as reflected in principal components analysis) using Offline Sorter (Plexon Inc.).

Neural Data Analyses

LFP Analyses—Spectral analyses implemented a multitaper fast Fourier transform method for calculating coherence and power (Bokil et al., 2010). Evaluation of statistically significant differences across conditions and subregions/subregion pairs in spectral measures by frequency was performed using a cluster based permutation approach similar to that described previously (Maris & Oostenveld, 2007), but adapted here to calculate F statistics (ANOVA) for more than a single independent variable and more than two levels of each variable. Non-normalized directed transfer function, also referred to as the transfer matrix (H), was calculated as the inverse of the fast Fourier-transformed multivariate autoregressive coefficient matrix (Kaminski & Blinowska, 1991).

Spiking Analyses—For all spiking analyses, only putative pyramidal (n = 448, 424, and 59 for CA3, CA1, subiculum, respectively) or granule (n= 104 for DG) neurons emitting at least 50 spikes across conditions were considered. Spike-LFP phase analyses were based on procedures in prior reports (Colgin et al., 2009; Mizuseki et al., 2012). Additionally, strength of phase modulation was assessed with pair-wise phase consistency (Vinck et al., 2010), which quantifies the consistency of angular phase preference for each possible pair of action potentials, thus avoiding the bias associated with mean resultant length.

Supplementary Material

Refer to Web version on PubMed Central for supplementary material.

Acknowledgments

We thank Max Farina for his assistance. This work was supported in part by NIH F31 grant MH102956 to J.B.T.

References

Ahmed OJ, Mehta MR. Running speed alters the frequency of hippocampal gamma oscillations. J Neurosci. 2012; 32:7373–7383. [PubMed: 22623683]

Amaral DG, Witter MP. The three-dimensional organization of the hippocampal formation: a review of anatomical data. Neuroscience. 1989; 31:571–591. [PubMed: 2687721]

Belchior H, Lopes-dos-Santos V, Tort AB, Ribeiro S. Increase in hippocampal theta oscillations during spatial decision making. Hippocampus. 2014; 24:693–702. [PubMed: 24520011]

Bender F, Gorbati M, Cadavieco MC, Denisova N, Gao X, Holman C, Korotkova T, Ponomarenko A. Theta oscillations regulate the speed of locomotion via a hippocampus to lateral septum pathway. Nature Com. 2015; 6:8521.

Bokil H, Andrews P, Kulkarni JE, Mehta S, Mitra PP. Chronux: a platform for analyzing neural signals. J Neurosci Methods. 2010; 192:146–151. [PubMed: 20637804]

Brovelli A, Ding M, Ledberg A, Chen Y, Nakamura R, Bressler SL. Beta oscillations in a large-scale sensorimotor cortical network: directional influences revealed by Granger causality. PNAS. 2004; 101:9849–9854. [PubMed: 15210971]

Burgess N, Maguire EA, O'Keefe J. The human hippocampus and spatial and episodic memory. Neuron. 2002; 35:625–641. [PubMed: 12194864]

Buzsáki G. Theta oscillations in the hippocampus. Neuron. 2002; 33:325–340. [PubMed: 11832222]

Buzsáki G, Anastassiou CA, Koch C. The origin of extracellular fields and currents—EEG, ECoG, LFP and spikes. Nature Rev Neurosci. 2012; 13:407–420. [PubMed: 22595786]

Clark RE, Squire LR. An animal model of recognition memory and medial temporal lobe amnesia: history and current issues. Neuropsychologia. 2010; 48:2234–2244. [PubMed: 20144894]

Colgin LL. Rhythms of the hippocampal network. Nature Rev Neurosci. 2016; 17:239–249. [PubMed: 26961163]

Colgin LL, Moser EI. Gamma oscillations in the hippocampus. Physiology. 2010; 25:319–329. [PubMed: 20940437]

Colgin LL, Denninger T, Fyhn M, Hafting T, Bonnevie T, Jensen O, Moser MB, Moser EI. Frequency of gamma oscillations routes flow of information in the hippocampus. Nature. 2009; 462:353–357. [PubMed: 19924214]

Davachi L. Item, context and relational episodic encoding in humans. Curr Opin Neurobiol. 2006; 16:693–700. [PubMed: 17097284]

Eichenbaum H, Dudchenko P, Wood E, Shapiro M, Tanila H. The hippocampus, memory, and place cells: is it spatial memory or a memory space? Neuron. 1999; 23:209–226. [PubMed: 10399928]

Engel AK, Fries P. Beta-band oscillations—signalling the status quo? Curr Opin Neurobiol. 2010; 20:156–165. [PubMed: 20359884]

Engel AK, Fries P, Singer W. Dynamic predictions: oscillations and synchrony in top–down processing. Nature Rev Neurosci. 2001; 2:704–716. [PubMed: 11584308]

Ennaceur A, Delacour J. A new one-trial test for neurobiological studies of memory in rats. 1: Behavioral data. Behav Brain Res. 1988; 31:47–59. [PubMed: 3228475]

Fries P, Reynolds JH, Rorie AE, Desimone R. Modulation of oscillatory neuronal synchronization by selective visual attention. Science. 2001; 291:1560–1563. [PubMed: 11222864]

Fries P. Rhythms for cognition: communication through coherence. Neuron. 2015; 88:220–235. [PubMed: 26447583]

Golani I, Benjamini Y, Eilam D. Stopping behavior: constraints on exploration in rats (Rattus norvegicus). Behav Brain Res. 1993; 53:21–33. [PubMed: 8466665]

Herrmann CS, Munk MH, Engel AK. Cognitive functions of gamma-band activity: memory match and utilization. Trends Cogn Sci. 2004; 8:347–355. [PubMed: 15335461]

Huerta PT, Lisman JE. Bidirectional synaptic plasticity induced by a single burst during cholinergic theta oscillation in CA1 in vitro. Neuron. 1995; 15:1053–1063. [PubMed: 7576649]

Hyman JM, Wyble BP, Goyal V, Rossi CA, Hasselmo ME. Stimulation in hippocampal region CA1 in behaving rats yields long-term potentiation when delivered to the peak of theta and long-term depression when delivered to the trough. J Neurosci. 2003; 23:11725–11731. [PubMed: 14684874]

Igarashi KM, Lu L, Colgin LL, Moser MB, Moser EI. Coordination of entorhinal-hippocampal ensemble activity during associative learning. Nature. 2014; 510:143–147. [PubMed: 24739966]

Jarrard LE. On the role of the hippocampus in learning and memory in the rat. Behav Neural Biol. 1993; 60:9–26. [PubMed: 8216164]

Jensen O, Kaiser J, Lachaux JP. Human gamma-frequency oscillations associated with attention and memory. Trends Neuro. 2007; 30:317–324.

Jutras MJ, Fries P, Buffalo EA. Gamma-band synchronization in the macaque hippocampus and memory formation. J Neurosci. 2009; 29:12521–12531. [PubMed: 19812327]

Jutras MJ, Fries P, Buffalo EA. Oscillatory activity in the monkey hippocampus during visual exploration and memory formation. PNAS. 2013; 110:13144–13149. [PubMed: 23878251]

Kaminski MJ, Blinowska KJ. A new method of the description of the information flow in the brain structures. Biological Cybern. 1991; 65:203–210.

Kemere C, Carr MF, Karlsson MP, Frank LM. Rapid and continuous modulation of hippocampal network state during exploration of new places. PLoS One. 2013; 8:e73114. [PubMed: 24023818]

Kesner RP, Rolls ET. A computational theory of hippocampal function, and tests of the theory: new developments. Neurosci & Biobehavl Rev. 2015; 48:92–147.

Kesner RP, Lee I, Gilbert P. A behavioral assessment of hippocampal function based on a subregional analysis. Rev Neurosci. 2004; 15:333–352. [PubMed: 15575490]

King C, Recce M, O'keefe J. The rhythmicity of cells of the medial septum/diagonal band of Broca in the awake freely moving rat: relationships with behaviour and hippocampal theta. Eur J Neurosci. 1998; 10:464–477. [PubMed: 9749709]

Knierim JJ, Lee I, Hargreaves EL. Hippocampal place cells: parallel input streams, subregional processing, and implications for episodic memory. Hippocampus. 2006; 16:755–764. [PubMed: 16883558]

Komorowski RW, Manns JR, Eichenbaum H. Robust conjunctive item–place coding by hippocampal neurons parallels learning what happens where. J Neurosci. 2009; 29:9918–9929. [PubMed: 19657042]

MacKay WA, Mendonca AJ. Field potential oscillatory bursts in parietal cortex before and during reach. Brain Res. 1995; 704:167–174. [PubMed: 8788911]

Malkova L, Mishkin M. One-trial memory for object-place associations after separate lesions of hippocampus and posterior parahippocampal region in the monkey. J Neurosci. 2003; 23:1956–1965. [PubMed: 12629201]

Manns JR, Eichenbaum H. Evolution of declarative memory. Hippocampus. 2006; 16:795–808. [PubMed: 16881079]

Maris E, Oostenveld R. Nonparametric statistical testing of EEG-and MEG-data. J Neurosci Methods. 2007; 164:177–190. [PubMed: 17517438]

McNaughton N, Ruan M, Woodnorth MA. Restoring theta-like rhythmicity in rats restores initial learning in the Morris water maze. Hippocampus. 2006; 16:1102–1110. [PubMed: 17068783]

Mizuseki K, Royer S, Diba K, Buzsáki G. Activity dynamics and behavioral correlates of CA3 and CA1 hippocampal pyramidal neurons. Hippocampus. 2012; 22(8):1659–1680. [PubMed: 22367959]

Montgomery SM, Buzsáki G. Gamma oscillations dynamically couple hippocampal CA3 and CA1 regions during memory task performance. PNAS. 2007; 104:14495–14500. [PubMed: 17726109]

Nicolelis MA, Baccala LA, Lin RC, Chapin JK. Sensorimotor encoding by synchronous neural ensembly activity at multiple levels of the somatosensory system. Science. 1995; 268:1353. [PubMed: 7761855]

Orr G, Rao G, Houston FP, McNaughton BL, Barnes CA. Hippocampal synaptic plasticity is modulated by theta rhythm in the fascia dentata of adult and aged freely behaving rats. Hippocampus. 2001; 11:647–654. [PubMed: 11811658]

Rangel LM, Chiba AA, Quinn LK. Theta and beta oscillatory dynamics in the dentate gyrus reveal a shift in network processing state during cue encounters. Front Sys Neuro. 2015:9.

Renner MJ, Seltzer CP. Molar characteristics of exploratory and investigatory behavior in the rat (Rattus norvegicus). J Comp Psychol. 1991; 105:326. [PubMed: 1778065]

Save E, Poucet B, Foreman N, Buhot MC. Object exploration and reactions to spatial and nonspatial changes in hooded rats following damage to parietal cortex or hippocampal formation. Behav Neurosci. 1992; 106:447. [PubMed: 1616611]

Shirvalkar PR, Rapp PR, Shapiro ML. Bidirectional changes to hippocampal theta–gamma comodulation predict memory for recent spatial episodes. PNAS. 2010; 107:7054–7059. [PubMed: 20351262]

Siegle JH, Wilson MA. Enhancement of encoding and retrieval functions through theta phase-specific manipulation of hippocampus. eLife. 2014; 3:e03061. [PubMed: 25073927]

Singer W. Neuronal synchrony: a versatile code for the definition of relations? Neuron. 1999; 24:49–65. [PubMed: 10677026]

Sławińska U, Kasicki S. The frequency of rat's hippocampal theta rhythm is related to the speed of locomotion. Brain Res. 1998; 796:327–331. [PubMed: 9689489]

Tallon-Baudry C, Bertrand O, Delpuech C, Pernier J. Oscillatory γ-band (30–70 Hz) activity induced by a visual search task in humans. J Neurosci. 1997; 17:722–734. [PubMed: 8987794]

Tiitinen HT, Sinkkonen J, Reinikainen K, Alho K, Lavikainen J, Näätänen R. Selective attention enhances the auditory 40-Hz transient response in humans. Nature. 1993; 364:59–60. [PubMed: 8316297]

Tort AB, Komorowski RW, Manns JR, Kopell NJ, Eichenbaum H. Theta–gamma coupling increases during the learning of item–context associations. PNAS. 2009; 106:20942–20947. [PubMed: 19934062]

Trimper JB, Stefanescu RA, Manns JR. Recognition memory and theta–gamma interactions in the hippocampus. Hippocampus. 2014; 24:341–353. [PubMed: 24227610]

Varela F, Lachaux JP, Rodriguez E, Martinerie J. The brainweb: phase synchronization and large-scale integration. Nature Rev Neuro. 2001; 2:229–239.

Vinck M, van Wingerden M, Womelsdorf T, Fries P, Pennartz CM. The pairwise phase consistency: a bias-free measure of rhythmic neuronal synchronization. Neuroimage. 2010; 51:112–122. [PubMed: 20114076]

Wang Y, Romani S, Lustig B, Leonardo A, Pastalkova E. Theta sequences are essential for internally generated hippocampal firing fields. Nature Neuro. 2015; 18:282–288.

Whishaw IQ, Gharbawie OA, Clark BJ, Lehmann H. The exploratory behavior of rats in an open environment optimizes security. Behav Brain Res. 2006; 171:230–239. [PubMed: 16678279]

Whishaw IQ, Vanderwolf CH. Hippocampal EEG and behavior: change in amplitude and frequency of RSA (theta rhythm) associated with spontaneous and learned movement patterns in rats and cats. Beh Biol. 1973; 8:461–484.

Winson J. Loss of hippocampal theta rhythm results in spatial memory deficit in the rat. Science. 1978; 201:160–163. [PubMed: 663646]

Witter MP, Wouterlood FG, Naber PA, Van Haeften T. Anatomical Organization of the Parahippocampal-Hippocampal Network. Ann N Y Acad Sci. 2000; 911:1–24. [PubMed: 10911864]

Zarnadze S, Bäuerle P, Santos-Torres J, Böhm C, Schmitz D, Geiger JRP, Dugladze T, Gloveli T. Cell-specific synaptic plasticity induced by network oscillations. eLife. 2016; 5:e14912. [PubMed: 27218453]

Zheng C, Bieri KW, Hwaun E, Colgin LL. Fast gamma rhythms in the hippocampus promote encoding of novel object-place pairings. eNeuro. 2016 ENEURO-0001.

Zheng C, Bieri KW, Trettel SG, Colgin LL. The relationship between gamma frequency and running speed differs for slow and fast gamma rhythms in freely behaving rats. Hippocampus. 2015; 25:924–938. [PubMed: 25601003]

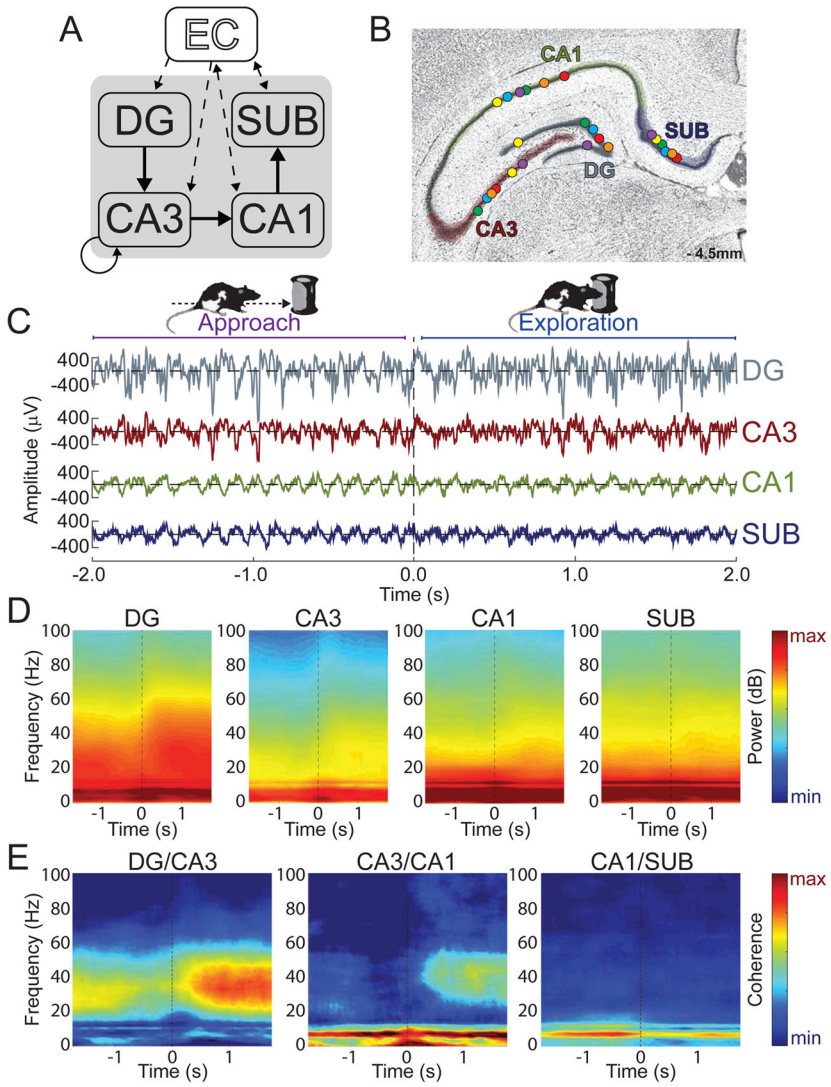

Figure 1. Slow gamma coherence increased while rats explored novel objects

(A) Illustration of the serial connections of the hippocampal subregions [DG, CA3, CA1, and SUB (subiculum)] as well as its connections with the entorhinal cortex (EC). **(B)** Coronal hippocampal section showing LFP recording locations (circles) for each rat (different colors) in each of the four targeted subregions. **(C)** Example LFP data as a rat approached (< 0 s) and explored (> 0 s) a novel object. **(D)** Moving window spectrograms for each hippocampal subregion time-locked to the initiation of novel object exploration (0 s). Minimum and maximum power values in decibels are noted on each spectrogram. **(E)** Moving window coherograms for each pair of directly connected hippocampal subregions time-locked to the initiation of novel object exploration (0 s). Increased coherence and power in the slow gamma range were apparent for DG/CA3 and CA3/CA1 during Exploration relative to Approach.

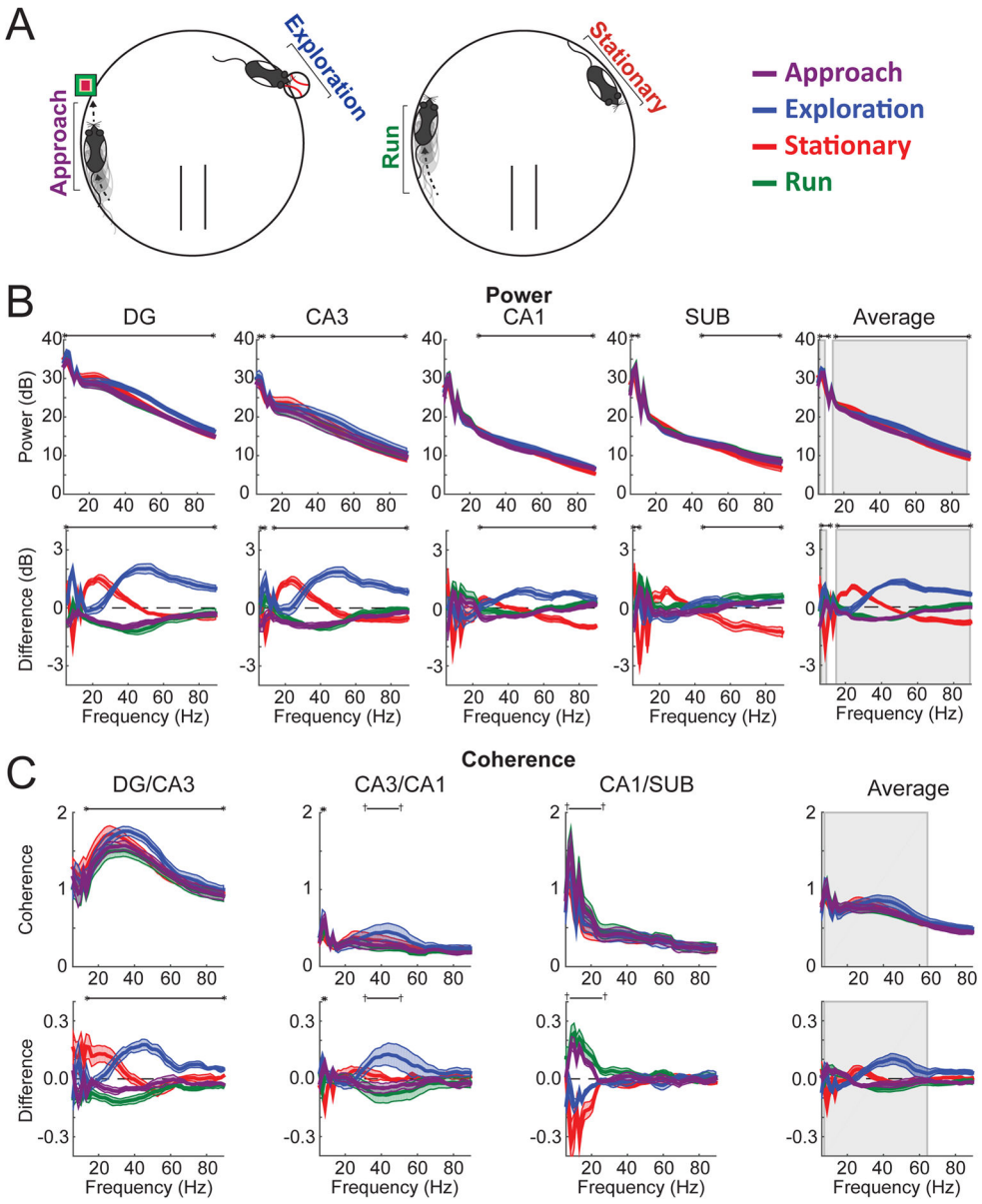

Figure 2. Object exploration was accompanied by a distinct spectral profile

(A) Illustration of the four behavioral states analyzed. **(B)** Top: Spectral power for each hippocampal subregion (and averaged across subregions) for each behavioral state. Bottom: Spectral power plotted as the difference from average across behavioral states. **(C)** Top: Coherence for each directly connected pair of hippocampal subregions (and averaged across subregion pairs). Bottom: Coherence plotted as the difference from average across behavioral states. Throughout the figure, gray rectangles mark frequency ranges exhibiting significant interactions between behavioral state and subregion. Black horizontal lines bookended by dagger symbols (†) indicate frequency ranges differing significantly ($p<.05$) across behavioral states, and those bookended by asterisks indicate significant differences after Bonferroni correction for multiple comparisons (here, 5 for power and 4 for

coherence). Colored lines indicate mean (darker shading) ± SEM (lighter shading). See also Figures S1, S2, and S3.

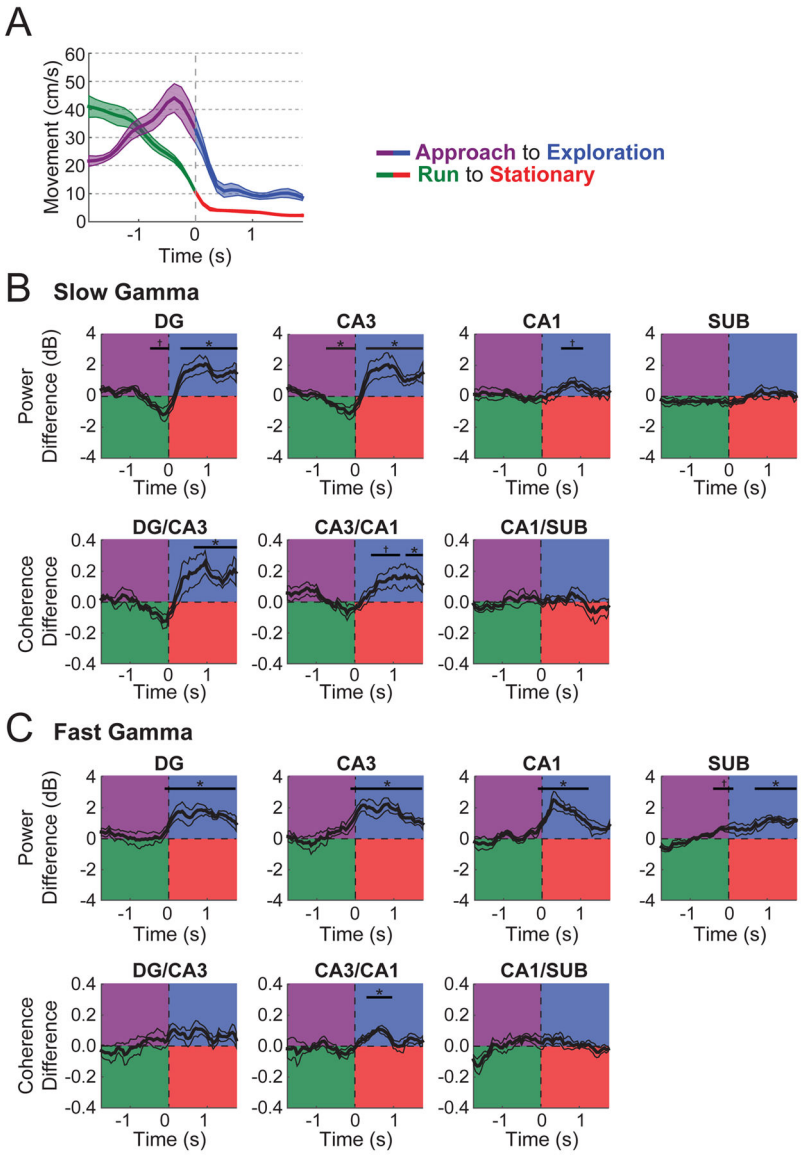

Figure 3. Gamma power and coherence during exploration was not explained as the product of the cessation of locomotion

(A) Speed of movement for 4-s epochs surrounding the transition from novel object Approach to Exploration (purple to blue) and from Run to Stationary (green to red). **(B)** Slow gamma power (top) and coherence (bottom) plotted as the difference between behavioral state transitions (Approach to Exploration minus Run to Stationary). For example, for CA3 slow gamma power, power was reduced for Approach relative to Run but increased during Exploration relative to Stationary. **(C)** Fast gamma power (top) and coherence (bottom) plotted as the difference between behavioral state transitions (Approach to Exploration minus Run to Stationary). Indicators of statistical significance throughout are the same as in Figure 2 except that Bonferroni-correction involved four and three comparisons here for power and coherence, respectively. Colored lines indicate mean (darker shading) ± SEM (lighter shading). See also Tables S1 and S2.

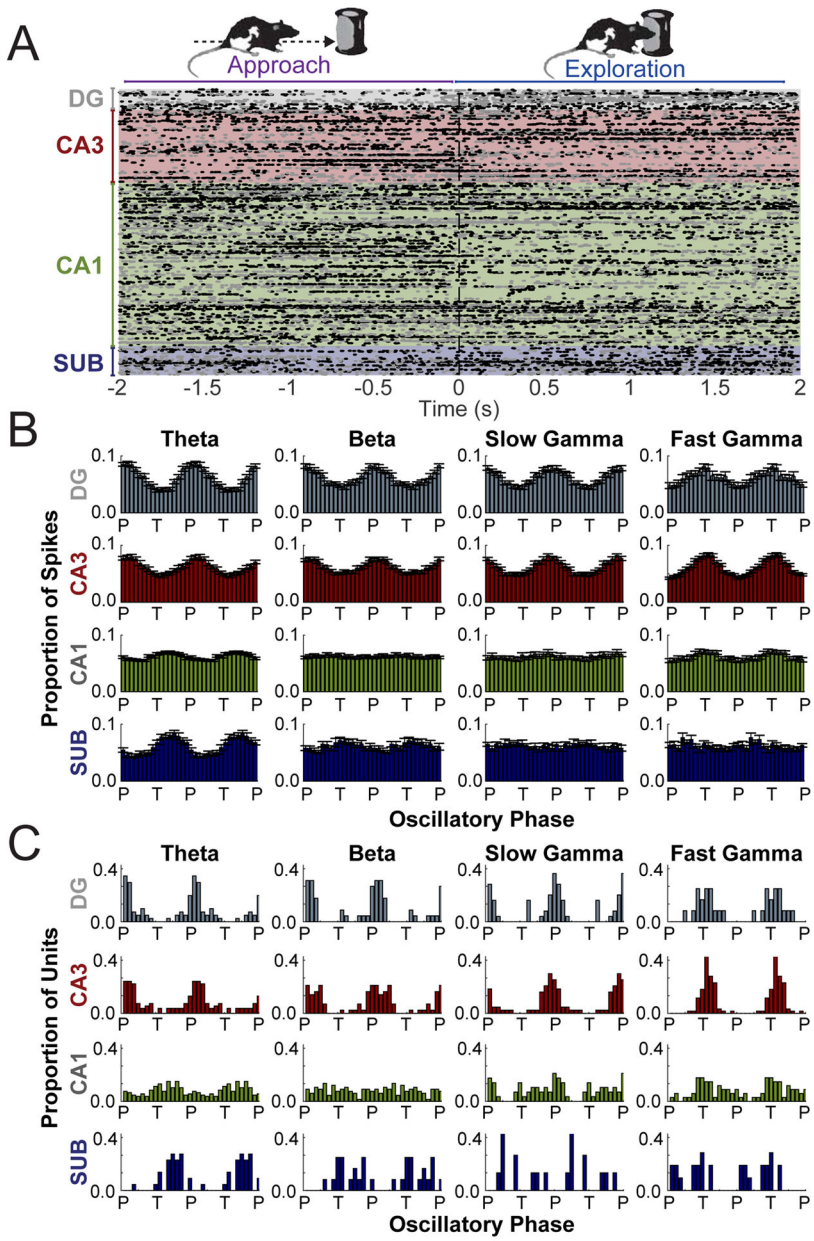

Figure 4. Principal cell firing aligned strongly to local oscillations in distinct frequency bands

(A) Peri-event raster of spike times by subregion time-locked to the initiation of object exploration events (0 s) [Approach (< 0 s); Exploration (> 0 s)]. Each dot indicates an action potential. Each row shows all action potentials from a single neuron. Rows alternate between gray and black dots for better visibility. **(B)** Mean distributions of action potentials in each subregion relative to the phase (P = peak; F = falling; T = trough; R = rising) of distinct oscillatory rhythms (denoted at top) recorded from that same subregion. Averages and error (SEM) are for those neurons found to be significantly phase modulated (see text). **(C)** Distributions across significantly phase modulated neurons of mean preferred oscillatory phase for spiking. Data is plotted twice in panels B and C, replicated across the oscillatory cycle, to aid visualization of periodicity. See also Figures S3, S4, and S5 and Table S3.

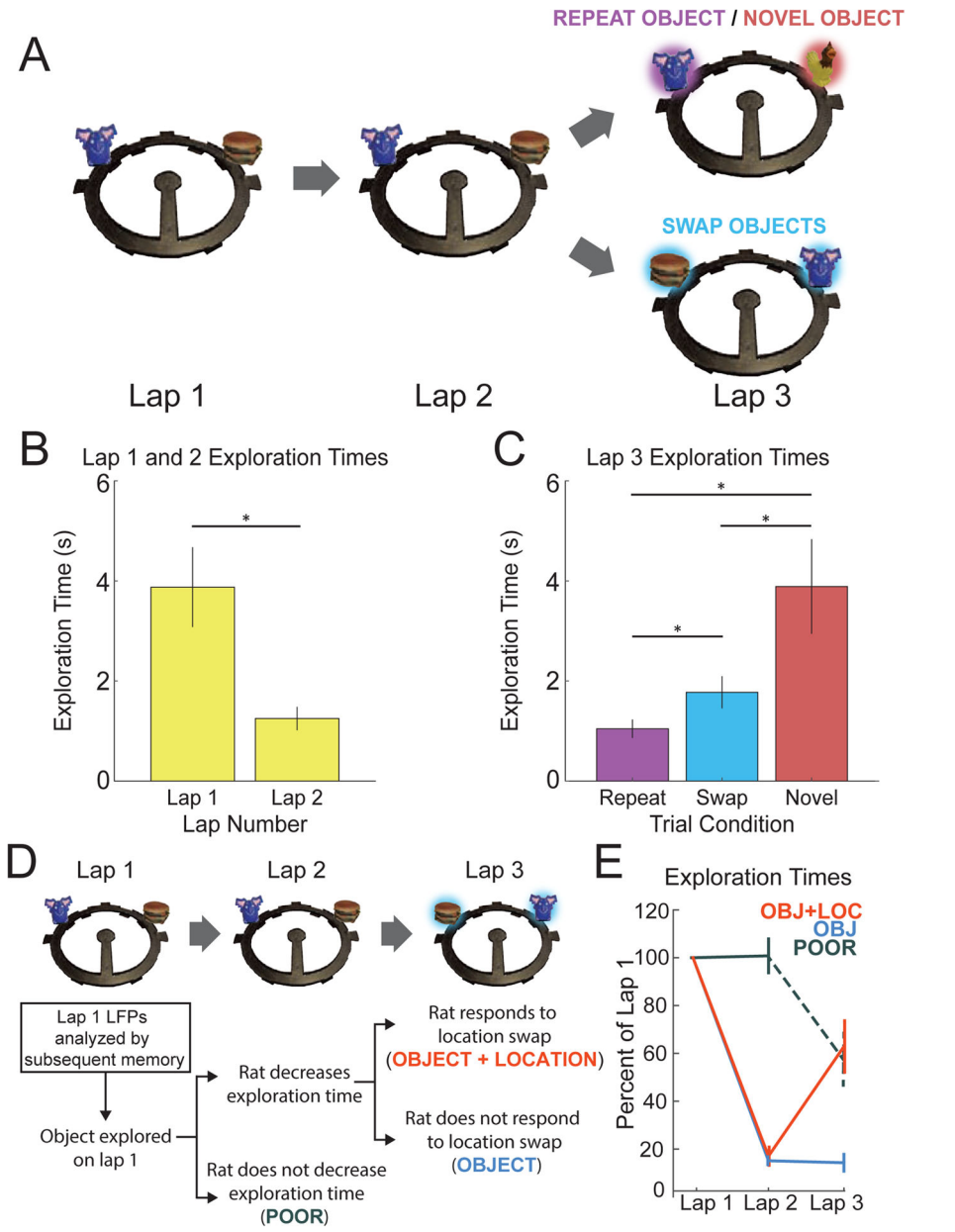

Figure 5. Rats demonstrated memory for objects and objects' locations

(A) Schematic of memory task. Each trial consisted of three laps around a circular track. On lap 1 of each trial, rats encountered two novel objects. On lap 2, rats encountered duplicates of those same two objects in the same positions. On lap 3, one of two trial-type manipulations were presented. Either: (1) one object was replaced with a duplicate while the other object was replaced by a novel object (REPEAT OBJECT/NOVEL OBJECT Trial) or (2) the objects were replaced by duplicates in swapped locations (SWAP OBJECTS Trial). **(B)** A significant reduction in average exploration time from lap 1 to lap 2 evidenced rats' memory for the novel objects presented on lap 1. Asterisks indicate $p<0.05$. **(C)** On lap 3, rats explored Novel objects longer than Swap objects, and Swap objects longer than Repeat objects, indicating memory for the objects' locations. Asterisks indicate $p<0.05$. **(D)**

Diagram of how object+location, object, and poor subsequent memory conditions were defined (also see Experimental Procedures). **(E)** Average exploration times across laps sorted by subsequent memory conditions and plotted as percent of lap 1 exploration time using colors indicated in panel D. Error bars throughout the figure show standard error of the mean across rats.

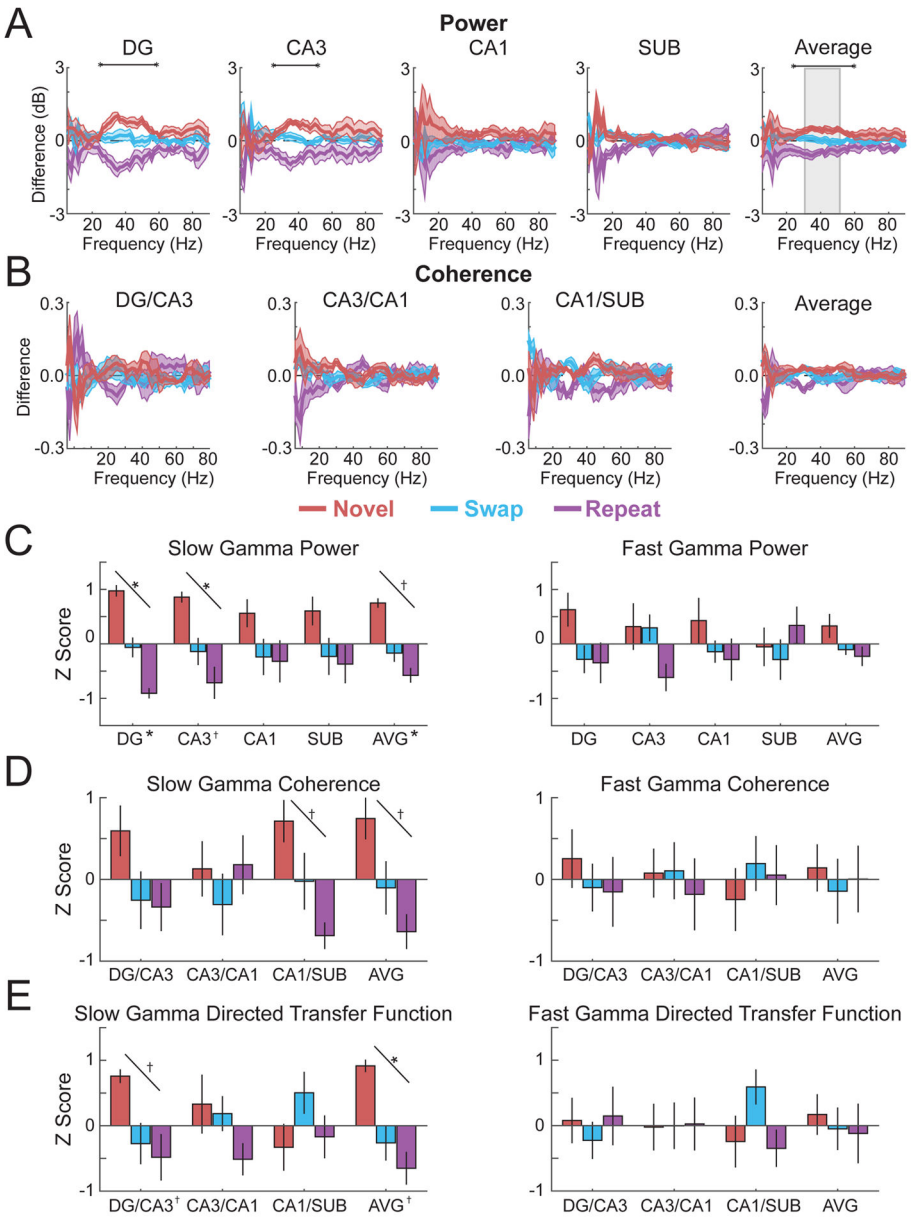

Figure 6. Slow gamma during lap 3 object exploration related to object-location memory condition

(A) Power by subregion (and the average across subregions) plotted as the difference from mean across memory conditions (denoted throughout figure by colors indicated in legend). **(B)** Coherence for each directly connected subregion pair plotted as the difference from mean across conditions. **(C)** Average slow gamma and fast gamma power for each subregion (and averaged across subregions; AVG) standardized to the mean across conditions and plotted as Z score. **(D)** Average slow gamma and fast gamma coherence for each directly connected subregion pair (and averaged across subregion pairs; AVG) standardized to the mean across conditions and plotted as Z score. **(E)** Average slow gamma and fast gamma non-normalized directed transfer function standardized to the mean across conditions and plotted as Z score. Colored lines in panels A and B indicate mean (darker shading) ± SEM

(lighter shading). Error bars in panels C, D, and E show SEM. Indicators of statistical significance in panels A and B are the same as in Figure 2. Similarly, diagonal lines in panels C, D, and E indicate statistical significance of linear trends, and symbols next the region labels on the x axes indicate statistical significance for that region of one-way repeated measures ANOVAs across object conditions. See also Figure S6 and Tables S4 and S5 for detailed statistics.

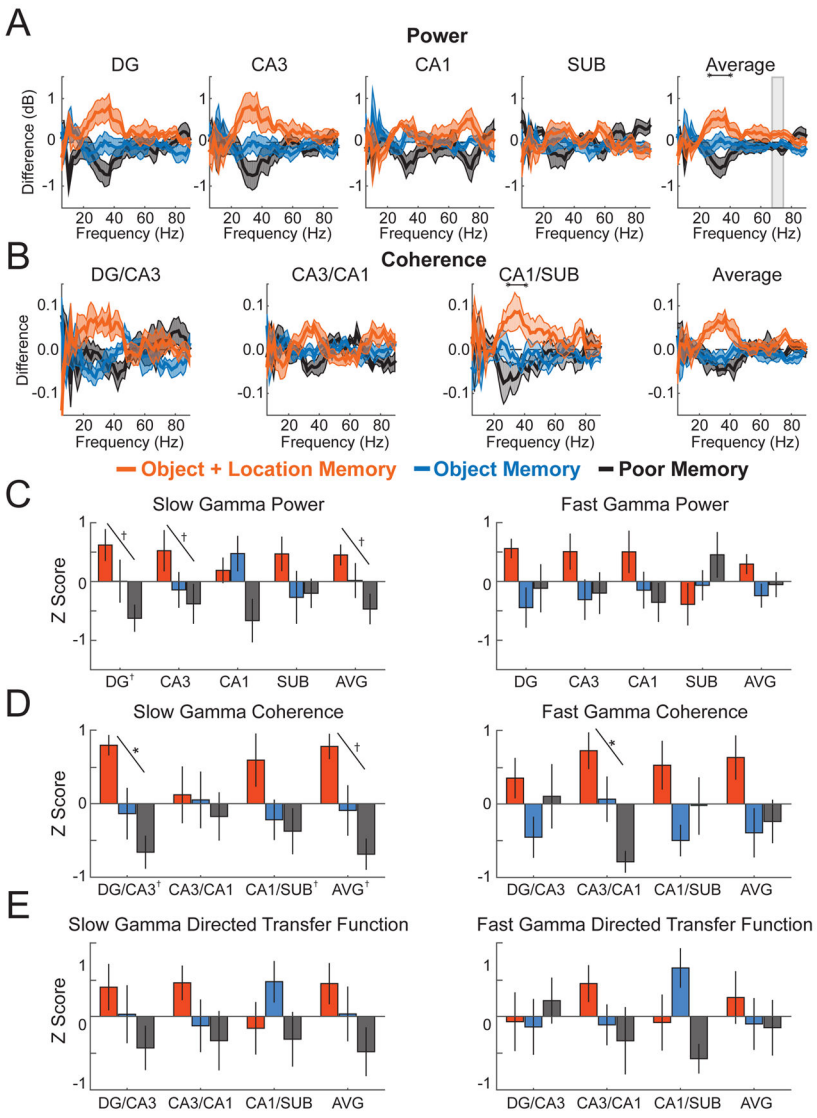

Figure 7. Slow gamma during novel object exploration related to subsequent object-location associative memory

(A) Power by subregion (and the average across subregions) plotted as the difference from mean across memory conditions (denoted throughout figure by colors indicated in legend). **(B)** Coherence for each directly connected subregion pair plotted as the difference from mean across conditions. **(C)** Average slow gamma and fast gamma power for each subregion (and averaged across subregions; AVG) standardized to the mean across conditions and plotted as Z score. **(D)** Average slow gamma and fast gamma coherence for each directly connected subregion pair (and averaged across subregion pairs; AVG) standardized to the mean across conditions and plotted as Z score. **(E)** Average slow gamma and fast gamma non-normalized directed transfer function standardized to the mean across conditions and plotted as Z score. Colored lines in panels A and B indicate mean (darker shading) ± SEM (lighter shading). Error bars in panels C, D, and E show SEM. Indicators of statistical significance in panels A and B are the same as in Figure 2. Similarly, diagonal lines in

panels C, D, and E indicate statistical significance of linear trends, and symbols next the region labels on the x axes indicate statistical significance for that region of one-way repeated measures ANOVAs across object conditions. See also Figure S7 and Tables S6 and S7 for detailed statistics.